PPARβ/δ prevents endoplasmic reticulum stress-associated inflammation and insulin resistance in skeletal muscle cells through an AMPK-dependent mechanism

Salvadó, Laia; Barroso, Emma; Gómez-Foix, Anna Maria; Palomer, Xavier; Michalik, Liliane; Wahli, Walter; Vázquez-Carrera, Manuel

2014

Salvadó, L., Barroso, E., Gómez-Foix, A. M., Palomer, X., Michalik, L., Wahli, W., et al. (2014). PPARβ/δ prevents endoplasmic reticulum stress-associated inflammation and insulin resistance in skeletal muscle cells through an AMPK-dependent mechanism. Diabetologia, 57(10), 2126-2135.

https://hdl.handle.net/10356/105878

https://doi.org/10.1007/s00125-014-3331-8

Article

PPARβ/δ prevents endoplasmic reticulum stress-associated inflammation and insulin resistance in skeletal muscle cells through an AMPK-dependent mechanism

Laia Salvadó[1,2], Emma Barroso[1,2], Anna Maria Gómez-Foix[2,3], Xavier Palomer[1,2], Liliane Michalik[4], Walter Wahli[4,5] and Manuel Vázquez-Carrera[1,2]

1. Department of Pharmacology and Therapeutic Chemistry, Faculty of Pharmacy, University of Barcelona, Institute of Biomedicine of the University of Barcelona (IBUB), Diagonal 643, E-08028 Barcelona, Spain

2. Spanish Biomedical Research Centre in Diabetes and Associated Metabolic Diseases (CIBERDEM), Spain, www.ciberdem.org

3. Department of Biochemistry and Molecular Biology, Faculty of Biology, University of Barcelona, IBUB, Barcelona, Spain

4. Center for Integrative Genomics, National Research Center Frontiers in Genetics, University of Lausanne, Lausanne, Switzerland

5. Lee Kong Chian School of Medicine, Nanyang Technological University, Singapore, Republic of Singapore

Corresponding author

M. Vázquez-Carrera, Department of Pharmacology and Therapeutic Chemistry, Faculty of Pharmacy, University of Barcelona, Diagonal 643, E-08028 Barcelona, Spain
E-mail: mvazquezcarrera@ub.edu

Received: 14 May 2014 / Accepted: 26 June 2014

Abstract

Aim/hypothesis Endoplasmic reticulum (ER) stress, which is involved in the link between inflammation and insulin resistance, contributes to the development of type 2 diabetes mellitus. In this study, we assessed whether peroxisome proliferator-activated receptor (PPAR)β/δ prevented ER stress-associated inflammation and insulin resistance in skeletal muscle cells.

Methods Studies were conducted in mouse C2C12 myotubes, in the human myogenic cell line LHCN-M2 and in skeletal muscle from wild-type and PPARβ/δ-deficient mice and mice exposed to a high-fat diet.

Results The PPARβ/δ agonist GW501516 prevented lipid-induced ER stress in mouse and human myotubes and in skeletal muscle of mice fed a high-fat diet. PPARβ/δ activation also prevented thapsigargin- and tunicamycin-induced ER stress in human and murine skeletal muscle cells. In agreement with this, PPARβ/δ activation prevented ER stress-associated inflammation and insulin resistance, and glucose-intolerant PPARβ/δ-deficient mice showed increased phosphorylated levels of inositol-requiring 1 transmembrane kinase/endonuclease-1α in skeletal muscle. Our findings demonstrate that PPARβ/δ activation prevents ER stress through the activation of AMP-activated protein kinase (AMPK), and the subsequent inhibition of extracellular-signal-regulated kinase (ERK)1/2 due to the inhibitory crosstalk between AMPK and ERK1/2, since overexpression of a dominant negative AMPK construct (K45R) reversed the effects attained by PPARβ/δ activation.

Conclusions/interpretation Overall, these findings indicate that PPARβ/δ prevents ER stress, inflammation and insulin resistance in skeletal muscle cells by activating AMPK.

Keywords

AMPK, ER stress, ERK1/2, NF-κB, PPAR β/δ

Abbreviations

2-DG	2-Deoxy-glucose
ACC2	Acetyl-CoA carboxylase 2
AMPK	AMP-activated protein kinase
ATF6	Activating transcription factor-6
eIF2α	Eukaryotic initiation factor 2α
EMSA	Electrophoretic mobility shift assay

ER	Endoplasmic reticulum
ERK	Extracellular signal-regulated kinase
IκB	Inhibitor of κB
IRE-1α	Inositol-requiring 1 transmembrane kinase/endonuclease-1α
NF-κB	Nuclear factor-κB
PERK	Eukaryotic translation initiation factor-2α kinase 3
PPAR	Peroxisome proliferator-activated receptor
UPR	Unfolded protein response
XBP1	X-box binding protein-1

Introduction

Insulin resistance, defined as a decrease in the action of insulin on target tissues [1], precedes and predicts the development of type 2 diabetes mellitus [2]. The primary site of insulin resistance in obesity and type 2 diabetes mellitus is skeletal muscle, since it accounts for the majority of insulin-stimulated glucose utilisation [3].

Recently, endoplasmic reticulum (ER) stress has emerged as a key player in the progression of insulin resistance and intersects with many different inflammatory and stress signalling pathways that disrupt insulin signalling [4]. The ER is responsible for the synthesis, folding and trafficking of secretory and membrane proteins. Disruption of ER homeostasis results in an adaptive unfolded protein response (UPR), intended to restore the ER's folding capacity and mitigate stress [5]. However, if ER stress is activated chronically, a decline in the action of insulin occurs, thus contributing to the development of type 2 diabetes mellitus [6]. Initiation of the canonical UPR involves activation of three key signalling proteins—inositol-requiring 1 transmembrane kinase/endonuclease-1α (IRE-1α), activating transcription factor-6 (ATF6) and eukaryotic translation initiation factor-2α kinase 3 (PERK). The endoribonuclease activity of IRE-1α cleaves a 26-base-pair segment from the mRNA of *XBP1*, creating the active (or spliced) form of the transcription factor *XBP1* (*sXBP1*). ATF6 translocates to the nucleus, in which it acts as a transcription factor and PERK phosphorylates and inhibits an essential initiator of translation, eukaryotic initiation factor 2α (eIF2α). Together, these pathways work to decrease translation and increase protein folding [7]. The three branches of the canonical UPR intersect with a variety of inflammatory and stress signalling systems, including the nuclear factor-κB (NF-κB) pathway [4], the activation of which has been linked with the impairment of insulin action in skeletal muscle

[8]. Thus, phosphorylation of eIF2α by PERK results in a general repression of mRNA translation. Since inhibitor of κB (IκB), which inhibits NF-κB, has a shorter half-life than NF-κB, UPR activation shifts the IκB/NF-κB ratio, thereby releasing NF-κB, which translocates to the nucleus and increases the expression of its target genes, such as *IL6* and *TNF* [9]. In addition, in response to ER stress, the cytoplasmatic domain of phosphorylated IRE1α can recruit TNF-α receptor-associated factor 2, forming a complex that interacts and activates IκB kinase, leading to NF-κB activation [9].

Activation of adenosine monophosphate-activated protein kinase (AMPK) exhibits multiple protective effects, including inhibition of inflammation and insulin resistance, and reduces the risk of developing type 2 diabetes mellitus [10]. Recently, it has been reported that AMPK activation protects against hypoxic injury [11], atherosclerosis [12, 13] and lipid-induced hepatic disorders [14] by reducing ER stress. Interestingly, an inhibitory crosstalk between AMPK and extracellular-signal-regulated kinase 1/2 (ERK1/2) has been reported [15] and inhibition of ERK1/2 was found to improve AMPK and Akt pathways and to reverse ER stress-induced insulin resistance in skeletal muscle cells [16].

Peroxisome proliferator-activated receptors (PPARs) are members of the nuclear receptor superfamily of ligand-inducible transcription factors [17] that may also suppress inflammation through diverse mechanisms [18–21]. Of the three PPAR isotypes found in mammals, PPARα [22] and PPARγ are the targets for fibrates and thiazolidinediones, respectively. Activation of the third isotype, PPARβ/δ, has been proposed as a potential treatment for insulin resistance [23] since it enhances fatty acid catabolism in adipose tissue and skeletal muscle [24, 25]. In fact, it has been reported that the increase in fatty acid oxidation in human skeletal muscle cells following treatment with the PPARβ/δ activator GW501516 is dependent on both PPARβ/δ and AMPK [26]. The present study was undertaken to determine whether PPARβ/δ prevents inflammation and insulin resistance in skeletal muscle cells by reducing ER stress.

Methods

Cell culture and mice Mouse C2C12 (ATCC, Manassas, VA) and human LHCN-M2 myoblasts were maintained, grown and differentiated to myotubes as previously described [27]. Lipid-containing media were prepared by conjugation of palmitic acid with fatty-acid-free BSA, as previously described [27]. For further details, please refer to the electronic supplementary material (ESM) Methods.

Five-week-old CD-1 male mice (Harlan Ibérica, Barcelona, Spain) were randomly distributed into three experimental groups (n = 8 each). One group was fed the standard diet, another was fed a western-type high-fat diet (HFD; 35% fat by weight, 58% energy from fat; Harlan Ibérica) plus one daily oral gavage of vehicle (0.5% wt/vol. carboxymethylcellulose) and the other was fed the HFD plus one daily oral dose of 3 mg kg^{-1} day^{-1} of the PPARβ/δ agonist GW501516 dissolved in the vehicle. After 3 weeks of treatment, mice were killed under isoflurane anaesthesia. Skeletal muscle (gastrocnemius) samples were frozen in liquid nitrogen and then stored at −80°C.
Male *Pparβ/δ* (also known as *Ppard*)-knockout mice and control mice (*Pparβ/δ*$^{+/+}$, wild-type) with the same genetic background (C57BL/6X129/SV), each having an initial weight of 20–25 g, were fed a standard diet. The generation of *Pparβ/δ*-null mice has been described previously [28]. All procedures were approved by the University of Barcelona Bioethics Committee, as stated in Law 5/21 July 1995 passed by the Generalitat de Catalunya.

RNA preparation and quantitative RT-PCR The relative levels of specific mRNAs were assessed by RT-PCR, as previously described [27]. Primer sequences used for RT-PCR are displayed in ESM Table 1.

Immunoblotting Isolation of total and nuclear extracts was performed as described elsewhere [27]. For further details, please refer to the ESM Methods.

Deoxy-D-glucose,2-[1,2-^{3}*H(N)] uptake experiments* 2-Deoxy-glucose (2-DG) uptake was performed as previously reported [27]. For further details, please refer to the ESM Methods.

Electrophoretic mobility shift assay An electrophoretic mobility shift assay (EMSA) was performed as previously described [27].

HPLC measurement of AMP The measurement of AMP using HPLC was performed as previously described [27]. For further details, please refer to the ESM Methods.

Statistical analyses Results are expressed as means ± SD. Significant differences were established by one-way ANOVA using the GraphPad Instat programme (GraphPad Software V5.01; GraphPad Software, San Diego, CA). When significant variations were found by one-way

ANOVA, the Tukey–Kramer multiple comparison post-hoc test was performed. Differences were considered significant at $p < 0.05$.

Results

PPARβ/δ activation prevents lipid-induced ER stress in mouse and human skeletal muscle cells To evaluate the effects of PPARβ/δ activation on palmitate-induced ER stress in skeletal muscle cells we first examined the effects of GW501516, a selective ligand for PPARβ/δ [29,30], on activated IRE1α. Palmitate exposure at 0.5 mmol/l induced an increase in the phosphorylated forms of IRE1α detected by slower migration, and this increase was almost completely prevented by treatment with GW501516 (Fig. 1a). Consistent with the increase in the phosphorylation status of IRE1α, which promotes the splicing of *Xbp1*, C2C12 myotubes exposed to 0.5 mmol/l palmitate showed increased spliced *Xbp1* (*sXbp1*) mRNA levels compared with cells exposed only to BSA (Fig. 1b), whereas in the presence of palmitate plus GW501516 the *sXbp1* mRNA levels were reduced. This effect of GW501516 was specific and PPARβ/δ dependent, since it was reversed by the PPARβ/δ antagonist GSK0660. In human LHCN-M2 myotubes (Fig. 1c) a similar trend was observed in *sXBP1* mRNA levels, indicating that the effect of GW501516 was not species specific. A similar profile of changes was observed when we examined the mRNA levels of several ER stress markers such as *Grp78/Bip* (also known as *Hspa5*), *Grp94* (also known as *Hsp90b1*) and *Orp150* (also known as *Hyou1*). Exposure to palmitate increased the expression of all these ER stress markers, whereas co-incubation with palmitate plus GW501516 led to a significant reduction (Fig. 1 d–f). Next, we evaluated whether PPARβ/δ activation protected against lipid-induced ER stress in vivo in skeletal muscle. We have previously reported that mice fed with an HFD were glucose-intolerant, whereas mice fed with the HFD and treated with GW501516 showed an improved response to glucose challenge [31]. In the skeletal muscle of these mice we observed that exposure to the HFD increased the phosphorylated forms of IRE1α and the protein levels of BIP compared with those in mice fed a standard diet, while these changes were prevented in HFD-fed mice treated with GW501516 (Fig. 1 g, h). Therefore, the improvement in glucose tolerance achieved by GW501516 in mice fed an HFD was accompanied by a reduction in the levels of ER stress markers in skeletal muscle.

PPARβ/δ activation prevents thapsigargin- and tunicamycin-induced ER stress in skeletal muscle cells To clearly demonstrate that PPARβ/δ activation prevents ER stress in skeletal muscle cells,

we then examined the effects of GW501516 on ER stress induced by thapsigargin, a potent ER stress inducer [32]. Thapsigargin elicited a huge increase in IRE1α protein levels, and GW501516 reduced the increase in the phosphorylated forms of this protein (Fig. 2a). Consistent with the effects of GW501516 on IRE1α, drug treatment downregulated the increase caused by thapsigargin in *sXbp1* transcript levels in murine (Fig. 2b) and human myotubes (Fig. 2c). GW501516 also significantly reduced the increase in the expression of other ER stress markers such as *CHOP* and *ATF3* in human myotubes (Fig. 2 d, e). Similarly, GW501516 significantly reduced the increase in mRNA levels in human (*CHOP* and *ATF3)* (Fig. 2 f, g) and murine (*Chop*, *Grp94* and *Orp150*) (Fig. 2 h–j) myotubes caused by another potent ER stress inducer, tunicamycin [31]. Overall, these findings demonstrate that PPARβ/δ activation prevents ER stress regardless of the inducer used.

PPARβ/δ activation prevents ER stress-induced inflammation and insulin resistance in skeletal muscle cells Given the association of ER stress with activation of the inflammatory process and insulin resistance [4,6], we next assessed whether PPARβ/δ activation reduced ER stress-associated inflammation and insulin resistance. First, we examined the NF-κB pathway. Thapsigargin reduced the protein levels of the NF-κB inhibitor IκBα [33] (Fig. 3a), whereas co-incubation of the cells with thapsigargin plus GW501516 led to an increase in the levels of this NF-κB inhibitor. Also, thapsigargin increased nuclear p65 subunit of NF-κB and co-incubation of the cells with thapsigargin plus the GW501516 prevented this increase (Fig. 3b). To clearly determine whether GW501516 prevented ER stress-induced inflammation, we measured NF-κB binding activity by EMSA. NF-κB formed one main complex with nuclear proteins (Fig. 3c). Specificity of the DNA-binding complex was assessed in competition experiments by adding an excess of unlabelled NF-κB oligonucleotide. NF-κB binding activity increased in nuclear extracts from thapsigargin- and tunicamycin-treated human cells, whereas in those cells co-incubated with these ER stressors and GW501516 the binding activity was similar to that in control cells. Addition of an antibody against the p65 and p50 subunits of NF-κB in thapsigargin-stimulated cells supershifted the complex, indicating that this band mainly consisted of these subunits. No supershift was observed after addition of an Oct-1 antibody, indicating that the NF-κB changes were specific. We then evaluated the effect of GW50156 on the expression of Tnf-α and IL-6, cytokines under the transcriptional control of NF-κB and which are also involved in insulin resistance [34, 35]. Consistent with the NF-κB findings, *Tnf* mRNA levels were increased in

C2C12 cells exposed to thapsigargin and Il6/*IL6* mRNA levels were increased in murine and human myotubes exposed to tunicamycin; co-incubation with GW501516 significantly reduced the expression of these cytokines (Fig. 3 d–f).

In an attempt to establish a relationship between PPARβ/δ and ER stress-induced insulin resistance we used *Pparβ/δ*-knockout mice. Interestingly, the PPARβ/δ-deficient mice showed glucose intolerance compared with wild-type mice (Fig. 4a) accompanied by an increase in the phosphorylated levels of IRE1α in skeletal muscle (Figure 4b). Moreover, in myotubes exposed to tunicamycin, we observed a reduction in insulin-stimulated Akt phosphorylation, which is consistent with the findings of previous studies (16, 27, 36). In cells co-incubated with tunicamycin plus GW501516 this effect was significantly reversed (Fig. 4c). Similarly, when we evaluated the protein levels of the insulin receptor β-subunit, which are reduced by defective insulin signalling [37], we observed a strong decrease following tunicamycin exposure; this response was attenuated by GW501516 (Fig. 4d). In concordance with these changes, tunicamycin reduced insulin-stimulated 2-DG uptake, whereas co-incubation with tunicamycin plus GW501516 restored a significant part of this reduction (Fig. 4e). Overall, these findings demonstrate that PPARβ/δ activation prevents ER stress-induced inflammation and insulin resistance in skeletal muscle cells.

PPARβ/δ modulates the crosstalk between AMPK and ERK pathways in skeletal muscle cells To assess the mechanism by which PPARβ/δ inhibits ER stress, we focused on the potential activation of AMPK by this nuclear receptor. AMPK, a pharmacological target for insulin resistance and type 2 diabetes mellitus [10], inhibits ER stress [11, 12, 14, 16] and its reduction promotes ER stress [13]. Interestingly, an inhibitory crosstalk between AMPK and ERK1/2 has been reported [15, 16] and inhibition of ERK1/2 improves AMPK and Akt signalling and reverses ER stress-induced insulin resistance in skeletal muscle cells [16]. To ascertain whether the effect of PPARβ/δ on ER stress involves this inhibitory crosstalk between AMPK and ERK1/2, we first examined the effects of the ER stressor tunicamycin on their phosphorylated protein levels. As shown in Fig. 5 a, b, tunicamycin reduced phospho-AMPK and increased phospho-ERK1/2 levels, which is in agreement with findings of previous studies [16] and suggests the presence of the inhibitory crosstalk between these kinases under our conditions. In addition, when cells were exposed to tunicamycin plus GW501516 or the MEK inhibitor U0126, the phosphorylation status of AMPK was increased compared with that in cells only exposed to tunicamycin (Fig. 5c). These findings

suggest that GW501516 might inhibit ERK1/2 through AMPK activation. Confirmation of the involvement of PPARβ/δ in ERK1/2 inhibition was supported by in vivo findings: skeletal muscle from PPARβ/δ-deficient mice showed increased phospho-ERK1/2 levels compared with wild-type mice (Fig. 5d). Moreover, exposure to an HFD increased phospho-ERK1/2 levels in skeletal muscle, whereas treatment of the HFD-fed mice with GW501516 reversed this increase (Fig. 5e). Likewise, when we analysed phospho-AMPK levels in the skeletal muscle of these mice we observed a trend in changes opposite to those observed for ERK1/2 (Fig. 5f).

PPARβ/δ prevents ER stress-induced inflammation and insulin resistance through an AMPK-dependent mechanism Because AMPK is activated allosterically by an increase in the intracellular AMP/ATP ratio [10], we measured adenine nucleotide concentrations in C2C12 cells to further investigate the underlying mechanism of GW501516 in AMPK activation. GW501516 significantly increased the AMP/ATP ratio (Fig. 6a), suggesting that this mechanism was responsible for the increase in AMPK activity following drug treatment. As a control for AMPK activity we measured phosphorylation of acetyl-CoA carboxylase 2 (ACC2), a substrate for AMPK [10]. In accordance with an increase in AMPK activity, ACC2 phosphorylation was increased following GW501516 treatment (Fig. 6b). In addition, our findings showed that the preventive effects of GW501516 on palmitate-induced ER stress in C2C12 myotubes were AMPK-dependent, since the reduction in *sXBP1* mRNA levels induced by GW501516 was reversed by the AMPK inhibitor compound C (Fig. 6c). Next, to confirm the involvement of AMPK in the effects of PPARβ/δ, we overexpressed an AMPKα subunit with a point mutation that causes the enzyme to function as a dominant negative suppressor of endogenous AMPK activity (K45R). Overexpression of this construct in C2C12 cells leads to the displacement of endogenous subunits, followed by degradation of the free α subunit [38]. Inhibition of AMPK activity attenuated the effect of GW501516 in tunicamycin-exposed cells on IκBα protein levels (Fig. 6d), insulin-stimulated Akt phosphorylation (Fig. 6e) and IRβ protein levels (Fig. 6f), suggesting that PPARβ/δ activation prevents ER stress-associated inflammation and insulin resistance through AMPK.

Discussion

Excessive ER stress contributes to the development of insulin resistance and type 2 diabetes mellitus [4, 6]. Therefore, reduction of ER stress may be critical in preventing these chronic

metabolic diseases. Findings from our study suggest that PPARβ/δ activation prevents ER stress-induced inflammation and insulin resistance in skeletal muscle cells and that some of the diabetes-protective and anti-inflammatory effects of the PPARβ/δ ligands might be due to their ability to reduce ER stress. Interestingly, the increase in ER stress markers in the skeletal muscle of *Pparβ/δ*-null mice indicates that this nuclear receptor offers protection against ER stress in this tissue, suggesting that a reduction in the activity of this nuclear receptor can exacerbate ER stress and its associated metabolic complications. Indeed, genetic variation in the *PPARβ/δ* gene predicts the conversion from impaired glucose tolerance to type 2 diabetes mellitus [39].

We have previously reported that PPARβ/δ activation prevented palmitate-induced inflammation and insulin resistance in skeletal muscle cells by increasing fatty acid oxidation in skeletal muscle cells [40]. Increased fatty acid oxidation following PPARβ/δ activation has also been reported to contribute to the reduction in palmitate-induced ER stress in pancreatic beta cells [41]. It has also been reported that PPARβ/δ activation prevents ethanol-induced ER stress in the liver [42] and in the aorta of high-fat, high-cholesterol-fed mice [43], although the mechanisms responsible for these effects have not been identified. In the present study we showed that PPARβ/δ activation prevents lipid-induced ER stress in vitro and in vivo in skeletal muscle cells, where the reported increase in fatty acid oxidation after PPARβ/δ activation may contribute to these effects. However, our data also demonstrate that PPARβ/δ activation prevents ER stress induced by potent ER stressors (either tunicamycin or thapsigargin), suggesting that the protective effect of PPARβ/δ on ER stress extends beyond increased fatty acid oxidation. In fact, our data show that PPARβ/δ activation inhibits ER stress through a mechanism involving AMPK activation. Targeting AMPK to prevent ER stress is consistent with previous studies reporting that AMPK activation reduces ER stress [11–14, 27]. Our findings also indicate that AMPK activation attained by PPARβ/δ activators is the result of an increase in the AMP/ATP ratio, which is in agreement with findings of previous studies [26, 31].

The findings of this study point to an additional mechanism by which PPARβ/δ activation may contribute to the increase in AMPK activity and the reduction in ER stress. This mechanism involves the inhibition of the ERK1/2 signalling pathway by PPARβ/δ. An inhibitory crosstalk exists between the AMPK and ERK1/2 pathways [15, 16] and recently it has been shown that ERK1/2 inhibition results in enhanced AMPK activity and prevention of ER stress-induced insulin resistance in myotubes [16]. In fact, ER stress significantly increases ERK1/2 phosphorylation in myotubes ([16] and this study), whereas ERK1/2 inhibition restores AMPK and insulin-stimulated

Akt phosphorylation caused by ER stress [16]. Our data demonstrate that PPARβ/δ activation prevents HFD-induced ERK1/2 phosphorylation and exhibits a trend to restore phospho-AMPK levels in skeletal muscle. These data suggest that PPARβ/δ regulates the inhibitory crosstalk between AMPK and ERK1/2 elicited by an HFD, causing an imbalance of this crosstalk in favour of AMPK, which prevents ER stress. The finding that *Pparβ/δ*-null mice show increased phospho-ERK1/2 levels in skeletal muscle clearly demonstrates that PPARβ/δ inhibits this pathway. This result is interesting since ERK1/2 is a potential drug target for preventing metabolic derangements. Thus, targeting ERK1/2 could protect obese mice against insulin resistance and liver steatosis by decreasing adipose tissue inflammation and increasing muscle glucose uptake [44].
In summary, on the basis of our findings we propose that PPARβ/δ prevents ER stress-associated inflammation and insulin resistance in skeletal muscle cells through AMPK activation.

Acknowledgements

We thank A. Orozco (Department of Biochemistry and Molecular Biology of the University of Barcelona, Spain) for experimental assistance with human myotube cultures. We thank M. J. Birnbaum (Howard Hughes Medical Institute, University of Pennsylvania, Philadelphia, PA, USA) for the pcDNA3/pAMPKalpha2-K45R plasmid.

Funding

This study was partly supported by funds from the Spanish Ministerio de Economía y Competitividad (SAF2009-06939 and SAF2012-30708) and the European Union ERDF. CIBER de Diabetes y Enfermedades Metabólicas Asociadas (CIBERDEM) is an Instituto de Salud Carlos III project. LS was supported by an FPI grant from the Spanish Ministerio de Economía y Competitividad. We thank the University of Barcelona's Language Advisory Service for revising the manuscript.

Contribution statement

LS, EB, AMG-F, XP, LM, WW and MV-C processed the samples, analysed and prepared the data and were involved in drafting the article. LS, EB, AG-F, XP, LM and WW contributed to the interpretation of the data and revised the article. MV-C and LS designed the experiments and analysed and interpreted the data. MV-C wrote the manuscript and is responsible for the integrity of the work as a whole. All authors approved the final version of the manuscript.

Duality of interest

The authors declare that there is no duality of interest associated with this manuscript.

References

1. Samuel VT, Shulman GI (2012) Mechanisms for insulin resistance: common threads and missing links. Cell 148: 852-871

2. Martin BC, Warram JH, Krolewski AS, Bergman RN, Soeldner JS, Kahn CR (1992) Role of glucose and insulin resistance in development of type 2 diabetes mellitus: results of a 25-year follow-up study. Lancet 340: 925-929

3. Kelley DE, Goodpaster BH, Storlien L (2002) Muscle triglyceride and insulin resistance. Annu Rev Nutr 22: 325-346

4. Hotamisligil GS (2010) Endoplasmic reticulum stress and the inflammatory basis of metabolic disease. Cell 140: 900-917

5. Ron D (2002) Translational control in the endoplasmic reticulum stress response. J Clin Invest 110: 1383-1388

6. Ozcan U, Cao Q, Yilmaz E, et al. (2004) Endoplasmic reticulum stress links obesity, insulin action, and type 2 diabetes. *Science* 306: 457-461

7. Eizirik DL, Cardozo AK, Cnop M (2008) The role for endoplasmic reticulum stress in diabetes mellitus. Endocr Rev 29: 42-61

8. Itani SI, Ruderman NB, Schmieder F, Boden G (2002) Lipid-induced insulin resistance in human muscle is associated with changes in diacylglycerol, protein kinase C, and IkappaB-alpha. Diabetes 51: 2005-2011

9. Zhang K, Kaufman RJ (2008) From endoplasmic-reticulum stress to the inflammatory response. Nature 454: 455-462

10. Zhang BB, Zhou G, Li C (2009) AMPK: an emerging drug target for diabetes and the metabolic syndrome. Cell Metab 9: 407-416

11. Terai K, Hiramoto Y, Masaki M, et al. (2005) AMP-activated protein kinase protects cardiomyocytes against hypoxic injury through attenuation of endoplasmic reticulum stress. Mol Cell Biol 25: 9554-9575

12. Dong Y, Zhang M, Wang S, et al. (2010) Activation of AMP-activated protein kinase inhibits oxidized LDL-triggered endoplasmic reticulum stress in vivo. Diabetes 59: 1386-1396

13. Dong Y, Zhang M, Liang B, et al. (2010) Reduction of AMP-activated protein kinase alpha2 increases endoplasmic reticulum stress and atherosclerosis in vivo. Circulation 121: 792-803
14. Wang Y, Wu Z, Li D, et al. (2011) Involvement of oxygen-regulated protein 150 in AMP-activated protein kinase-mediated alleviation of lipid-induced endoplasmic reticulum stress. J Biol Chem 286: 11119-11131
15. Du J, Guan T, Zhang H, Xia Y, Liu F, Zhang Y (2008) Inhibitory crosstalk between ERK and AMPK in the growth and proliferation of cardiac fibroblasts. Biochem Biophys Res Commun 368: 402-407
16. Hwang SL, Jeong YT, Li X, et al. (2013) Inhibitory cross-talk between the AMPK and ERK pathways mediates endoplasmic reticulum stress-induced insulin resistance in skeletal muscle. Br J Pharmacol 169: 69-81
17. Michalik L, Auwerx J, Berger JP, et al. (2006) International Union of Pharmacology. LXI. Peroxisome proliferator-activated receptors. Pharmacol Rev 58: 726-741
18. Lee CH, Chawla A, Urbiztondo N, et al. (2003) Transcriptional repression of atherogenic inflammation: modulation by PPARdelta. Science 302: 453-457
19. Pascual G, Fong AL, Ogawa S, et al. (2005) A SUMOylation-dependent pathway mediates transrepression of inflammatory response genes by PPAR-gamma. Nature 437: 759-763
20. Daynes RA, Jones DC (2002) Emerging roles of PPARs in inflammation and immunity. Nat Rev Immunol 2: 748-759
21. Devchand PR, Keller H, Peters JM, Vazquez M, Gonzalez FJ, Wahli W (1996) The PPARalpha-leukotriene B4 pathway to inflammation control. Nature 384: 39-43
22. Auwerx J, Baulieu E, Beato M, et al. (1999) A unified nomenclature system for the nuclear receptor superfamily. *Cell* 97: 161-163
23. Schuler M, Ali F, Chambon C, et al. (2006) PGC1alpha expression is controlled in skeletal muscles by PPARbeta, whose ablation results in fiber-type switching, obesity, and type 2 diabetes. Cell Metab 4: 407-414
24. Lee CH, Olson P, Hevener A, et al. (2006) PPARdelta regulates glucose metabolism and insulin sensitivity. Proc Natl Acad Sci U S A. 103: 3444-3449
25. Barish GD, Narkar VA, Evans RM (2006) PPAR delta: a dagger in the heart of the metabolic syndrome. J Clin Invest 116: 590-597
26. Krämer DK, Al-Khalili L, Guigas B, Leng Y, Garcia-Roves PM, Krook A (2007) Role of AMP kinase and PPARdelta in the regulation of lipid and glucose metabolism in human skeletal muscle. J Biol Chem 282: 19313-19320

27. Salvadó L, Coll T, Gómez-Foix AM, et al. (2013) Oleate prevents saturated-fatty-acid-induced ER stress, inflammation and insulin resistance in skeletal muscle cells through an AMPK-dependent mechanism. Diabetologia 56: 1372-1382
28. Nadra K, Anghel SI, Joye E, et al. (2006) Differentiation of trophoblast giant cells and their metabolic functions are dependent on peroxisome proliferator-activated receptor beta/delta. Mol Cell Biol 26: 3266-3281
29. Oliver WR Jr, Shenk JL, Snaith MR, et al. (2001) A selective peroxisome proliferator-activated receptor delta agonist promotes reverse cholesterol transport. Proc Natl Acad Sci U S A 98: 5306-5311
30. Kino T., Rice KC, Chrousos GP (2007) The PPARβ/δ agonist GW501516 supresses interleukin 6-mediated hepatocyte acute phase reaction via STAT3 inhibition. Eur J Clin Invest 37: 425-433.
31. Barroso E, Rodríguez-Calvo R, Serrano-Marco L, et al. (2011) The PPARβ/δ activator GW501516 prevents the down-regulation of AMPK caused by a high-fat diet in liver and amplifies the PGC-1α-Lipin 1-PPARα pathway leading to increased fatty acid oxidation. Endocrinology 152: 1848-1859
32. Xu C, Bailly-Maitre B, Reed JC (2005) Endoplasmic reticulum stress: cell life and death decisions. J Clin Invest 115: 2656-2664
33. Weigert C, Brodbeck K, Staiger H, et al. (2004) Palmitate, but not unsaturated fatty acids, induces the expression of interleukin-6 in human myotubes through proteasome-dependent activation of nuclear factor-kappaB. J Biol Chem;279:23942-23952.
35. Kern PA, Ranganathan S, Li C, Wood L, Ranganathan G (2001) Adipose tissue tumor necrosis factor and interleukin-6 expression in human obesity and insulin resistance. Am J Physiol Endocrinol.Metab 280: E745-E751
36. Pickup JC, Mattock MB, Chusney GD, Burt D (1997) NIDDM as a disease of the innate immune system: association of acute-phase reactants and interleukin-6 with metabolic syndrome X. Diabetologia 40: 1286-1292
37. Hage Hassan R, Hainault I, Vilquin JT, et al. (2012) Endoplasmic reticulum stress does not mediate palmitate-induced insulin resistance in mouse and human muscle cells. Diabetologia 55: 204-214
38. Liang CP, Han S, Okamoto H, et al. (2004) Increased CD36 protein as a response to defective insulin signaling in macrophages. J Clin Invest 113: 764-773

39. Mu J, Brozinick JT, Valladares O, Bucan M, Birnbaum MJ (2001) A role for AMP-activated protein kinase in contraction- and hypoxia-regulated glucose transport in skeletal muscle. Mol Cell 7: 1085-1094
40. Andrulionyte L, Peltola P, Chiasson JL, Laakso M, STOP-NIDDM Study Group (2006) Single nucleotide polymorphisms of PPARD in combination with the Gly482Ser substitution of PGC-1A and the Pro12Ala substitution of PPARG2 predict the conversion from impaired glucose tolerance to type 2 diabetes: the STOP-NIDDM trial. Diabetes 55: 2148-2152
41. Coll T, Alvarez-Guardia D, Barroso E, et al. (2010) Activation of peroxisome proliferator-activated receptor-δ by GW501516 prevents fatty acid-induced nuclear factor-κB activation and insulin resistance in skeletal muscle cells. Endocrinology 151: 1560-1569
42. Cao M, Tong Y, Lv Q, et al. (2012) PPARδ Activation RESCUES PAncreatic β-cell line INS-1E from palmitate-induced endoplasmic reticulum stress through enhanced fatty acid oxidation. PPAR Res. 2012: 680684
43. Ramirez T, Tong M, Chen WC, Nguyen QG, Wands JR, de la Monte SM (2013) Chronic alcohol-induced hepatic insulin resistance and endoplasmic reticulum stress ameliorated by peroxisome-proliferator activated receptor-δ agonist treatment. J Gastroenterol Hepatol. 28: 179-187
44. Bojic LA, Burke AC, Chokker SS, et al. (2014) Peroxisome Proliferator-Activated Receptor d agonist GW1516 attenuates diet-induced aortic inflammation, insulin resistance, and atherosclerosis in low-density lipoprotein receptor knockout mice. Arterioscler Thromb Vasc Biol 34: 52-60.
45. Jager J, Corcelle V, Grémeaux T, et al. (2011) Deficiency in the extracellular signal-regulated kinase 1 (ERK1) protects leptin-deficient mice from insulin resistance without affecting obesity. Diabetologia 54: 180-189.

Figure legends

Fig. 1 PPARβ/δ activation prevents lipid-induced ER stress in skeletal muscle cells. C2C12 or LHCN-M2 myotubes were incubated for 16 h in the absence (Ct, Control) or presence of palmitate (Pal) (0.3 or 0.5 mmol/l for C2C12 and 0.25 mmol/l for LHCN-M2) with or without pretreatment (before palmitate exposure) with 10 μmol/l GW501516 (GW) for 24 h or with 10 μmol/l GSK0660 (GSK) for 30 min. (**a**) Cell lysates from C2C12 cells exposed to BSA (Ct) or to 0.3 mmol/l or 0.5 mmol/l Pal were subjected to western blot analysis with antibody against IRE-1α. (**b**, **c**) *sXbp1* mRNA levels in C2C12 (**b**) and LHCN-M2 (**c**) myotubes. (**d**–**f**) mRNA levels of *Bip* (**d**), *Grp94* (**e**) and *Orp150* (**f**) in C2C12 myotubes. (**g**, **h**) Skeletal muscle lysates from mice fed a standard chow diet (Ct) or an HFD with or without GW (3 mg kg^{-1} day^{-1}) were subjected to western blot analysis with antibodies against IRE1α (**g**) and BIP (**h**). ***p<0.001 and *p<0.05 vs control; $^{\dagger\dagger\dagger}p$<0.001 and $^{\dagger\dagger}p$<0.01 vs palmitate-exposed cells or HFD-exposed mice. sXBP1: spliced XBP1. uXBP1: unspliced XBP1.

Fig. 2 PPARβ/δ activation prevents thapsigargin- and tunicamycin-induced ER stress in myotubes. C2C12 or LHCN-M2 myotubes were incubated for 16 h in the absence (Ct, Control) or presence of thapsigargin (Thapsi) (1 μmol/l for C2C12 and 100 nmol/l for LHCN-M2) or 2 or 5 μg/ml tunicamycin (Tuni) with or without pretreatment with 10 μmol/l GW501516 (GW) for 24 h. (**a**) Cell lysates were subjected to western blot analysis with antibody against IRE-1α. (**b**, **c**) mRNA levels of *sXbp1* in C2C12 (**b**) and LHCN-M2 (**c**) myotubes. (**d**–**g**) mRNA levels of *CHOP* (**d**, **f**) and *ATF3* (**e**, **g**) in LHCN-M2 myotubes exposed to 100 nmol/l Thapsi (**d**, **e**) or 2 μg/ml Tuni (**f**, **g**) with or without pretreatment with 10 μmol/l GW for 24 h. (**h**–**j**) mRNA levels of *Chop* (**h**), *Grp94* (**i**) and *Orp150* (**j**) in C2C12 myotubes exposed to 2 or 5 μg/ml Tuni with or without pretreatment with 10 μmol/l GW for 24 h. ***p<0.001 vs control; †† <0.01 and $^{\dagger\dagger\dagger}p$<0.001 vs Thapsi- or Tuni-treated cells. sXBP1: spliced XBP1. uXBP1: unspliced XBP1.

Fig. 3 PPARβ/δ activation prevents ER stress-induced inflammation in skeletal muscle cells. C2C12 or LHCN-M2 myotubes were incubated for 16 h or 2 h (EMSA) in the absence (Ct, Control) or presence of 1 μmol/l thapsigargin (Thapsi) or 2 μg/ml tunicamycin (Tuni) with or without pretreatment with 10 μmol/l GW501516 (GW) for 24 h. (**a**, **b**) Cell lysates were subjected to western blot analysis with antibody against IκBα (**a**) or the p65 subunit of NF-κB (**b**). The

graphs represent the quantification of the normalised protein levels expressed as a percentage of control samples ± SD. (**c**) Autoradiograph of EMSA performed with a ^{32}P-labelled NF-κB nucleotide and crude nuclear protein extract (NE) from LHCN-M2 myotubes. One main specific complex (I) based on competition with a molar excess of unlabelled probe is shown. The supershift immune complex (IC) obtained by incubating NE with an antibody (Ab) directed against the p65 and p50 subunits of NF-κB is also shown. (**d**–**f**) mRNA levels of *Tnf* (**d**) and murine *Il6* (**e**) and human *IL6* (**f**). *p<0.05, **p<0.01 and ***p<0.001 vs control; $^{\dagger}p$<0.05, $^{\dagger\dagger}p$<0.01 and $^{\dagger\dagger\dagger}p$<0.001 vs Thapsi- or Tuni-treated cells

Fig. 4 PPARβ/δ activation prevents ER stress-induced insulin resistance in skeletal muscle cells. (**a**) Glucose tolerance test (and AUC) in wild-type (WT) and *Pparβ/δ*-null (KO) mice. Data are expressed as means ± SD (n=9 mice per group). (**b**) Skeletal muscle cell lysates from WT and KO mice were subjected to western blot analysis with antibodies against total and phospho-IRE-1α. (**c**–**e**) C2C12 myotubes were incubated for 16 h in the absence (Ct, Control) or the presence of 0.5 μg/ml tunicamycin (Tuni) with or without pretreatment with 10 μmol/l GW501516 (GW) for 24 h. When indicated, cells were incubated with 100 nmol/l insulin (Ins) for the last 10 min. C2C12 cell lysates were subjected to western blot analysis with antibodies against total and phospho-Akt (Ser473) (**c**) and insulin receptor β-subunit (IRβ) (**d**). 2-DG uptake was assessed without or with insulin (**e**). *p<0.05 and **p<0.01 vs WT mice, control cells or control cells not exposed to insulin; $^{\dagger}p$<0.05 and $^{\dagger\dagger\dagger}p$<0.001 vs insulin-stimulated control cells or cells incubated with tunicamycin; $^{\ddagger}p$<0.05 and $^{\ddagger\ddagger}p$<0.01 vs insulin-stimulated cells incubated with tunicamycin

Fig. 5 PPARβ/δ modulates the crosstalk between AMPK and ERK pathways in skeletal muscle cells. C2C12 myotubes were incubated for 16 h in the absence (Ct, Control) or presence of 5 μg/ml tunicamycin (Tuni) with or without pretreatment with 10 μmol/l GW501516 (GW) or 10 μmol/l U0126 for 24 h. (**a**–**c**) C2C12 cell lysates subjected to western blot analysis with antibodies against total and phospho-AMPK (Thr^{172}) (**a**, **c**) and total and phospho-ERK1/2 (**b**). (**d**) Skeletal muscle cell lysates from wild-type (WT) and *Pparβ/δ*-null (KO) mice were subjected to western blot analysis with antibodies against total and phospho-ERK1/2. (**e**, **f**) Skeletal muscle lysates from mice fed a standard chow diet (Ct) or an HFD with or without GW501516 (3 mg kg^{-1} day^{-1}) were subjected to western blot analysis with antibodies against total and phospho-ERK1/2 (**e**) and total

and phospho-AMPK (**f**). *p<0.05 vs control cells, WT mice or mice fed with chow diet; $^{\dagger}p$<0.05 and $^{\dagger\dagger}p$<0.01 vs Tuni-exposed cells or mice fed an HFD

Fig. 6 PPARβ/δ prevents ER stress through an AMPK-dependent mechanism. (**a**) AMP/ATP ratio in C2C12 myotubes incubated for 16 h in the absence (Ct, Control) or presence of 0.5 mmol/l palmitate (Pal) with or without pretreatment with 10 μmol/l GW501516 (GW) for 24 h. (**b**) Cell lysates were subjected to western blot analysis with antibodies against total and phospho-ACC2. *p<0.05 and **p<0.001 vs cells exposed to palmitate alone. (**c**) *sXBP1* mRNA levels in LHCN-M2 myotubes incubated for 16 h in the absence (Ct, Control) or presence of 0.25 mmol/l Pal with or without pretreatment with 10 μmol/l GW or 10 μmol/l compound C (Cc) for 24 h. (**d**–**f**) C2C12 myotubes transfected with LacZ- or pAMPKα2 K45R-carrying plasmids (AMPK-DN) were incubated for 16 h in the absence (Ct, Control) or presence of 0.5 μg/ml tunicamycin (Tuni) with or without pretreatment with 10 μmol/l GW. Cell lysates were subjected to western blot analysis with antibodies against IκBα (**d**) total and phospho-Akt (Ser^{473}) (**e**) and IRβ (**f**). When indicated, cells were incubated with 100 nmol/l insulin (Ins) for the last 10 min. Data are expressed as mean ± SD. *p<0.05 and ***p<0.001 vs LacZ cells, LacZ+Ins-treated cells; $^{\dagger}p$<0.05 vs Tuni-exposed cells; $^{\ddagger}p$<0.05 and $^{\ddagger\ddagger\ddagger}p$<0.001 vs cells co-incubated with Tuni plus GW; $^{\S\S\S}p$<0.001 vs LacZ cells not exposed to Ins

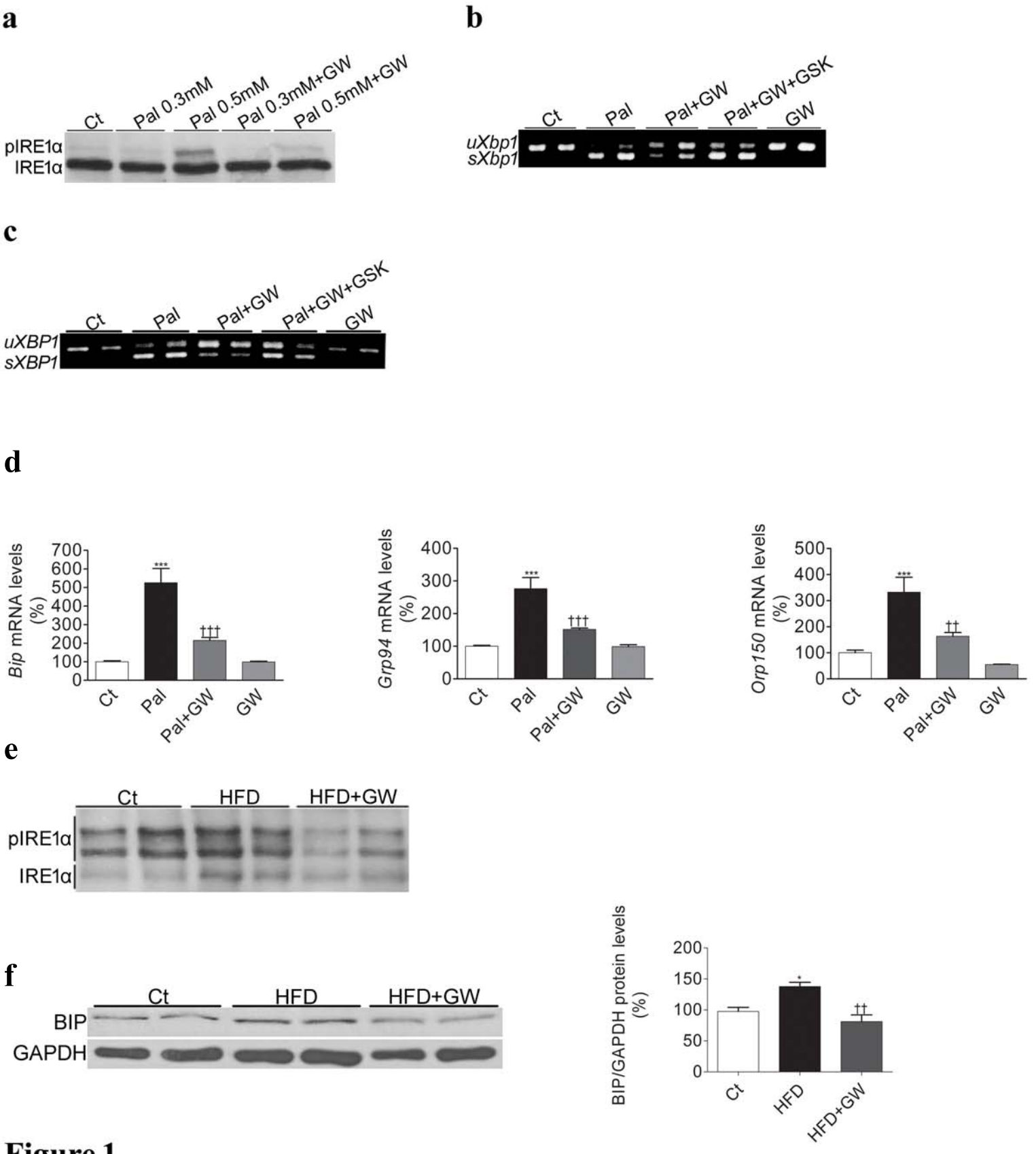
a
Ct
Pal 0.3mM
Pal 0.5mM
Pal 0.3mM+GW
Pal 0.5mM+GW
pIRE1α
IRE1α
b
Ct
Pal
Pal+GW
Pal+GW+GSK
GW
uXbp1
sXbp1
c
Ct
Pal
Pal+GW
Pal+GW+GSK
GW
uXBP1
sXBP1
d
Bip mRNA levels (%)
Grp94 mRNA levels (%)
Orp150 mRNA levels (%)
Ct
Pal
Pal+GW
GW
e
Ct
HFD
HFD+GW
pIRE1α
IRE1α
f
Ct
HFD
HFD+GW
BIP
GAPDH
BIP/GAPDH protein levels (%)

Figure 1

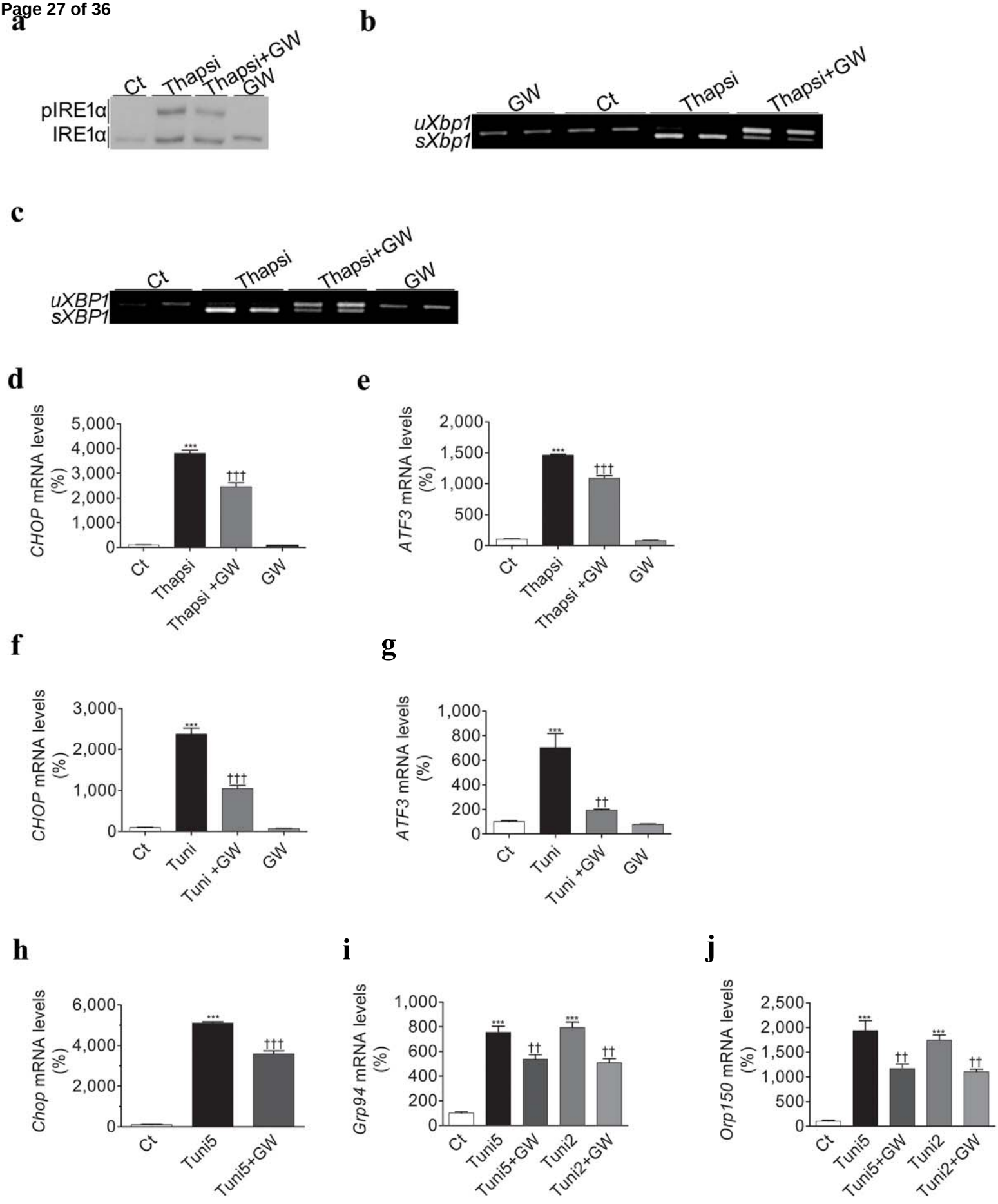
a
Ct
Thapsi
Thapsi+GW
GW
pIRE1α
IRE1α
b
GW
Ct
Thapsi
Thapsi+GW
uXbp1
sXbp1
c
Ct
Thapsi
Thapsi+GW
GW
uXBP1
sXBP1
d
CHOP mRNA levels (%)
5,000
4,000
3,000
2,000
1,000
0
***
†††
Ct
Thapsi
Thapsi +GW
GW
e
ATF3 mRNA levels (%)
2,000
1,500
1,000
500
0
***
†††
Ct
Thapsi
Thapsi +GW
GW
f
CHOP mRNA levels (%)
3,000
2,000
1,000
0
***
†††
Ct
Tuni
Tuni +GW
GW
g
ATF3 mRNA levels (%)
1,000
800
600
400
200
0
***
††
Ct
Tuni
Tuni +GW
GW
h
Chop mRNA levels (%)
6,000
4,000
2,000
0
***
†††
Ct
Tuni5
Tuni5+GW
i
Grp94 mRNA levels (%)
1,000
800
600
400
200
0
***
††
***
††
Ct
Tuni5
Tuni5+GW
Tuni2
Tuni2+GW
j
Orp150 mRNA levels (%)
2,500
2,000
1,500
1,000
500
0
***
††
***
††
Ct
Tuni5
Tuni5+GW
Tuni2
Tuni2+GW

Figure 2

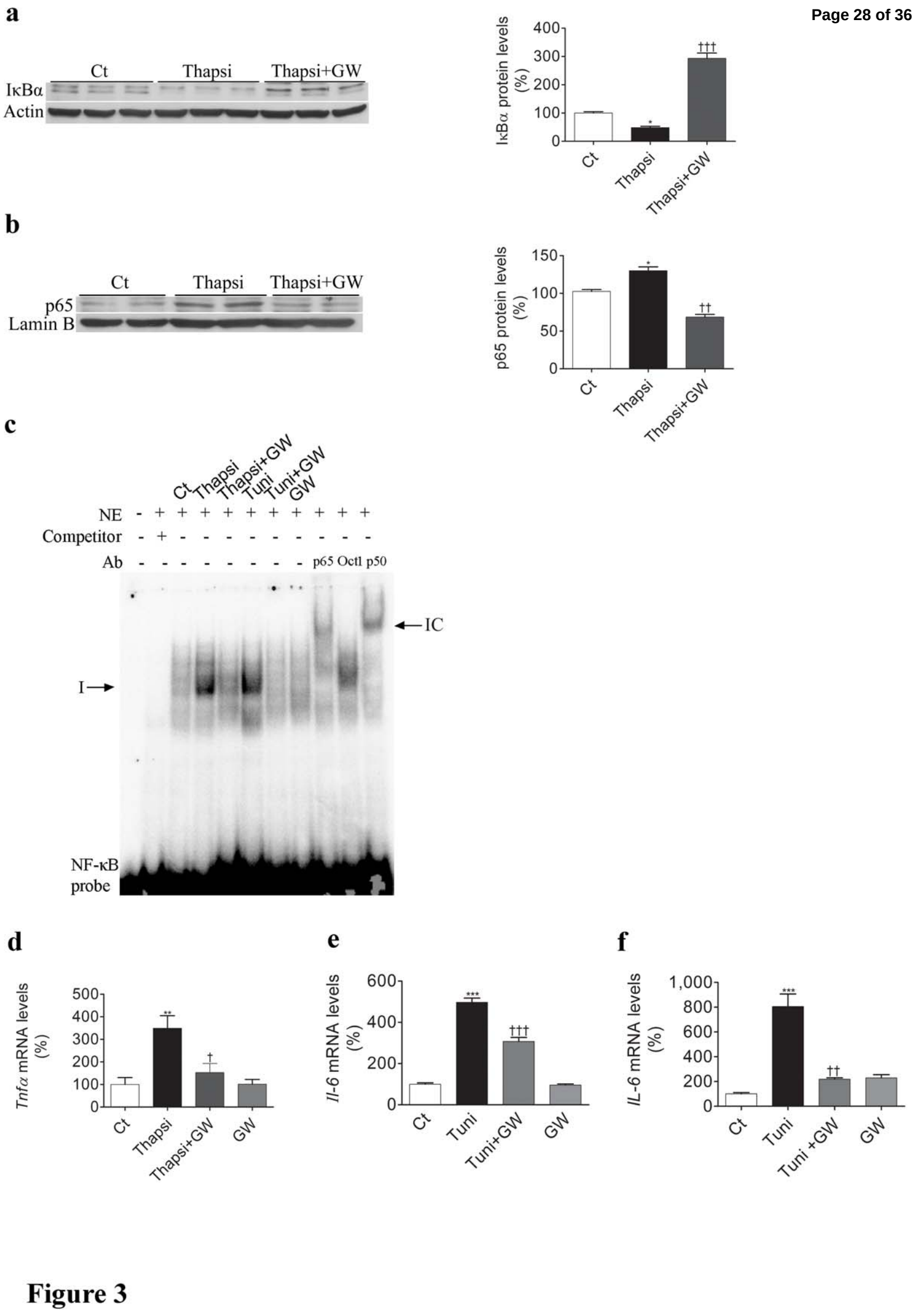
a
Ct
Thapsi
Thapsi+GW
IκBα
Actin
IκBα protein levels (%)
400
300
200
100
0
*
†††
Ct
Thapsi
Thapsi+GW
b
Ct
Thapsi
Thapsi+GW
p65
Lamin B
p65 protein levels (%)
150
100
50
0
*
††
Ct
Thapsi
Thapsi+GW
c
Ct
Thapsi
Thapsi+GW
Tuni
Tuni+GW
GW
NE - + + + + + + + + + +
Competitor - + - - - - - - - - -
Ab - - - - - - - - p65 Oct1 p50
IC
I
NF-κB probe
d
Tnfα mRNA levels (%)
500
400
300
200
100
0
**
†
Ct
Thapsi
Thapsi+GW
GW
e
Il-6 mRNA levels (%)
600
400
200
0
***
†††
Ct
Tuni
Tuni+GW
GW
f
IL-6 mRNA levels (%)
1,000
800
600
400
200
0
***
††
Ct
Tuni
Tuni +GW
GW

Figure 3

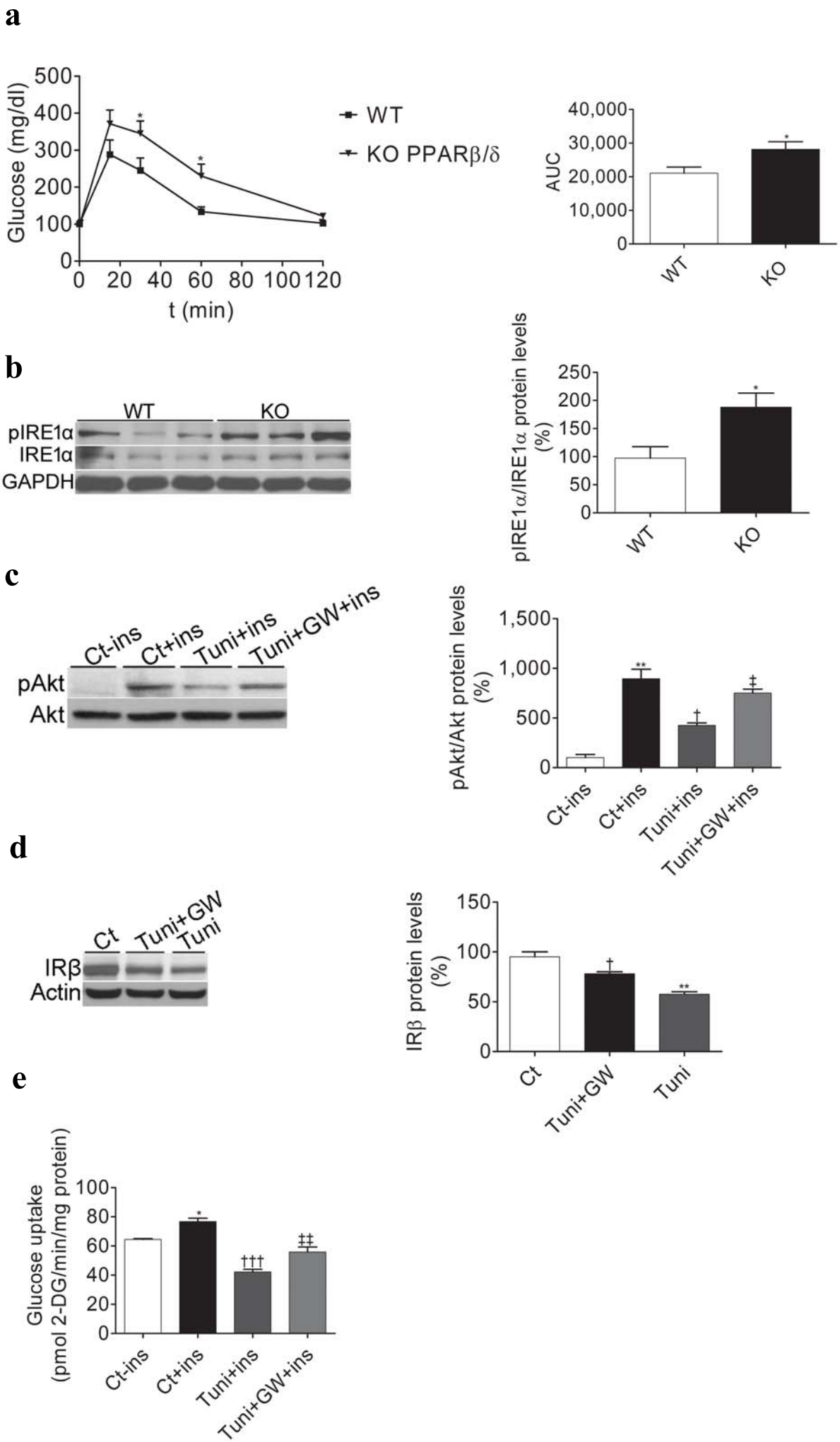
a
Glucose (mg/dl)
t (min)
WT
KO PPARβ/δ
AUC
WT
KO
b
WT
KO
pIRE1α
IRE1α
GAPDH
pIRE1α/IRE1α protein levels (%)
WT
KO
c
Ct-ins
Ct+ins
Tuni+ins
Tuni+GW+ins
pAkt
Akt
pAkt/Akt protein levels (%)
Ct-ins
Ct+ins
Tuni+ins
Tuni+GW+ins
d
Ct
Tuni+GW
Tuni
IRβ
Actin
IRβ protein levels (%)
Ct
Tuni+GW
Tuni
e
Glucose uptake (pmol 2-DG/min/mg protein)
Ct-ins
Ct+ins
Tuni+ins
Tuni+GW+ins

Figure 4

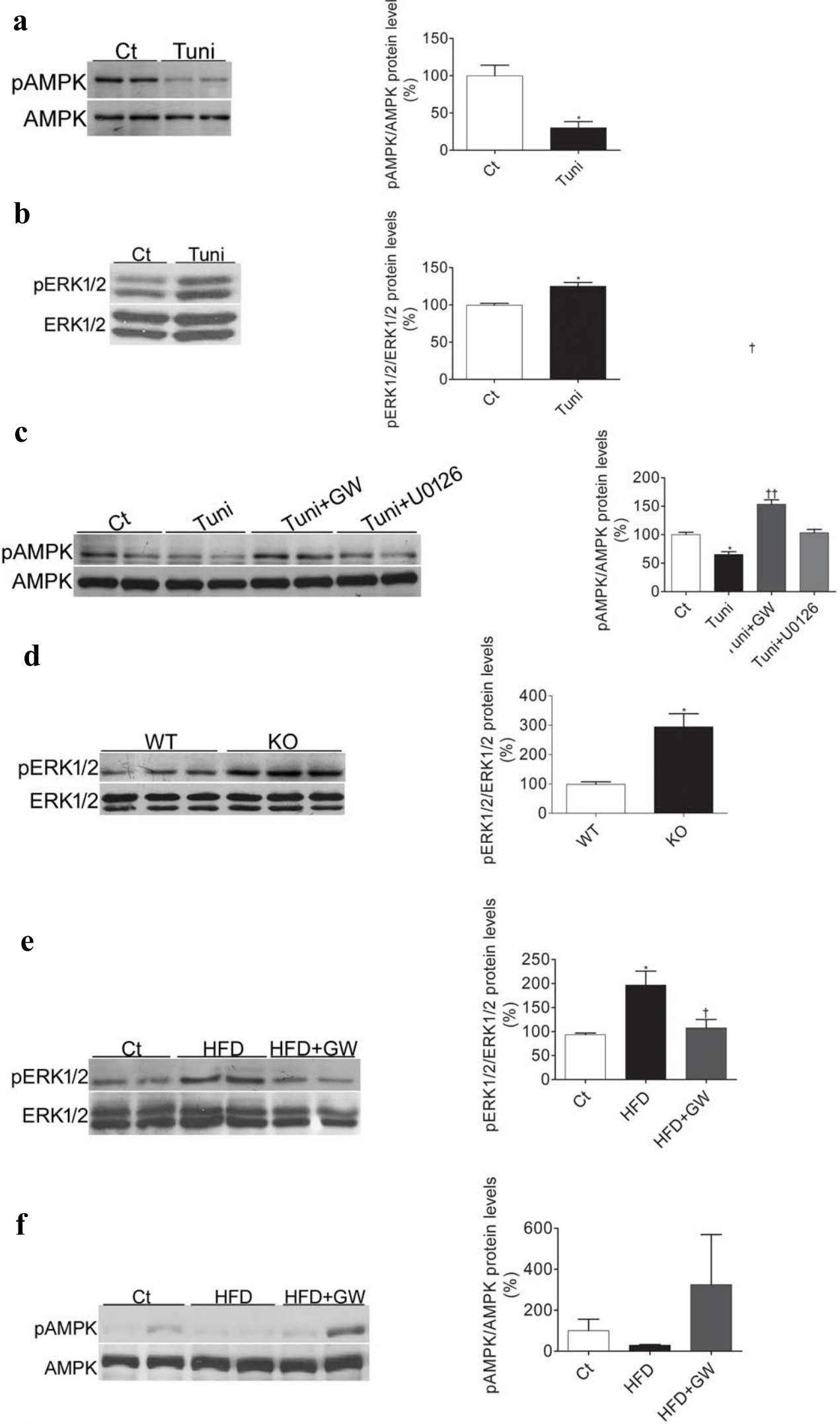
a
Ct
Tuni
pAMPK
AMPK
pAMPK/AMPK protein levels (%)
150
100
50
0
Ct
Tuni
b
Ct
Tuni
pERK1/2
ERK1/2
pERK1/2/ERK1/2 protein levels (%)
150
100
50
0
Ct
Tuni
c
Ct
Tuni
Tuni+GW
Tuni+U0126
pAMPK
AMPK
pAMPK/AMPK protein levels (%)
200
150
100
50
0
Ct
Tuni
Tuni+GW
Tuni+U0126
d
WT
KO
pERK1/2
ERK1/2
pERK1/2/ERK1/2 protein levels (%)
400
300
200
100
0
WT
KO
e
Ct
HFD
HFD+GW
pERK1/2
ERK1/2
pERK1/2/ERK1/2 protein levels (%)
250
200
150
100
50
0
Ct
HFD
HFD+GW
f
Ct
HFD
HFD+GW
pAMPK
AMPK
pAMPK/AMPK protein levels (%)
600
400
200
0
Ct
HFD
HFD+GW

Figure 5

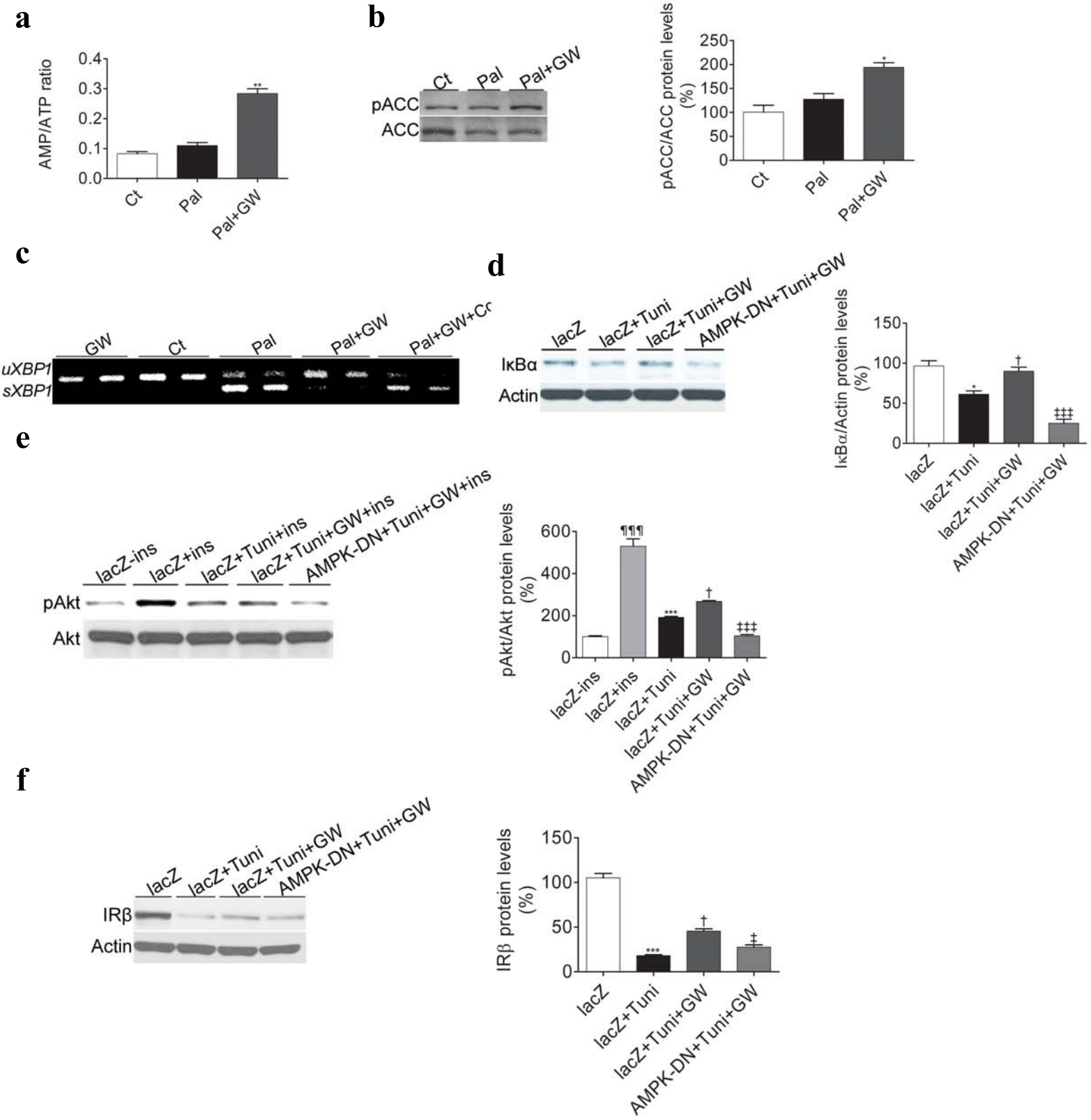
a
AMP/ATP ratio
0.4
0.3
0.2
0.1
0.0
**
Ct
Pal
Pal+GW
b
Ct
Pal
Pal+GW
pACC
ACC
pACC/ACC protein levels (%)
250
200
150
100
50
0
*
Ct
Pal
Pal+GW
c
GW
Ct
Pal
Pal+GW
Pal+GW+Cc
uXBP1
sXBP1
d
lacZ
lacZ+Tuni
lacZ+Tuni+GW
AMPK-DN+Tuni+GW
IκBα
Actin
IκBα/Actin protein levels (%)
150
100
50
0
*
†
‡‡‡
lacZ
lacZ+Tuni
lacZ+Tuni+GW
AMPK-DN+Tuni+GW
e
lacZ-ins
lacZ+ins
lacZ+Tuni+ins
lacZ+Tuni+GW+ins
AMPK-DN+Tuni+GW+ins
pAkt
Akt
pAkt/Akt protein levels (%)
600
400
200
0
¶¶¶
***
†
‡‡‡
lacZ-ins
lacZ+ins
lacZ+Tuni
lacZ+Tuni+GW
AMPK-DN+Tuni+GW
f
lacZ
lacZ+Tuni
lacZ+Tuni+GW
AMPK-DN+Tuni+GW
IRβ
Actin
IRβ protein levels (%)
150
100
50
0
***
†
‡
lacZ
lacZ+Tuni
lacZ+Tuni+GW
AMPK-DN+Tuni+GW

Figure 6

Electronic supplementary material (ESM)-Methods

Cell culture and mice Mouse C2C12 myoblasts (ATCC) were maintained in Dulbecco's modified Eagle's medium (DMEM) supplemented with 10% fetal bovine serum (FBS) and 1% penicillin/streptomycin (10.000 units/ml of penicillin and 10.000 µg/ml of streptomycin). When cells reached confluence, the medium was switched to the differentiation medium containing DMEM and 2% horse serum, which was changed every other day. After four additional days, the differentiated C2C12 cells had fused into myotubes. Lipid-containing media were prepared by conjugation of palmitic acid with fatty acid-free bovine serum albumin, as previously described [1]. Following incubation, RNA or protein were extracted from myotubes as described below.

The human myogenic cell line LHCN-M2 was grown in DMEM:Medium 199 (4:1) supplemented with 15% FBS, 16 mM HEPES, 30 ng/ml zinc sulphate, 1.4 µg/ml vitamin B12, 55 ng/ml dexamethasone, 5 ng/ml hepatocyte growth factor and 2.5 ng/ml fibroblast growth factor. To induce differentiation to myotubes, when cells reached 80-90% confluence the medium was changed to DMEM: Medium 199 (4:1) supplemented with 0.5% FBS, 20 mmol/l HEPES, 10 µg/ml insulin, 100 µg/ml apo-transferrin and 55 ng/ml dexamethasone for two days, and then to DMEM:Medium 199 (4:1) supplemented with 0.5% FBS, 20 mmol/l HEPES and 55 ng/ml dexamethasone for three additional days [1].

Mice were maintained under standard conditions of illumination (12-h light/dark cycle) and temperature (21±1ºC), and were fed a standard diet before the studies began. Food and water were provided ad libitum. The research complied with the Guide for the Care and Use of Laboratory Animals published by the US National Institutes of Health (NIH Publication No. 85-23, revised 1996). All procedures were approved by the University of Barcelona Bioethics Committee, as stated in Law 5/21 July 1995 passed by the Generalitat de Catalunya.

Before the end of the treatments, a glucose tolerance test was performed on mice fasted for 4h. Animals received 2 g/Kg body weight of glucose by intraperitoneal injection and blood was collected from the tail vein after 0, 15, 30, 60 and 120 minutes.

The research complied with the Guide for the Care and Use of Laboratory Animals published by the US National Institutes of Health (NIH Publication No. 85-23, revised 1996). All procedures were approved by the University of Barcelona Bioethics Committee, as stated in Law 5/21 July 1995 passed by the Generalitat de Catalunya.

Immunoblotting To obtain total proteins, myotubes were homogenized in RIPA lysis buffer (Sigma) with 5 mmol/l NaF, 1 mmol/l phenylmethylsulfonyl fluoride, 10 mmol/l sodium orthovanadate and 5.4 μg/mL aprotinin at 4ºC for 30 min. The homogenate was centrifuged at 17,000 g for 30 min at 4ºC. Protein concentration was measured by the Bradford method. Total proteins (30 μg) were separated by SDS-PAGE on 10% separation gels and transferred to Immobilon polyvinylidene difluoride membranes (Millipore, Bedford, MA). In the case of IRE-1α a phos-tag gel was used as previously described [1]. Western blot analysis was performed using antibodies against total and phospho-Akt (Ser^{473}), total and phospho-AMPK (Thr^{172}), total and phospho-ACC2, total and phospho-ERK1/2 (Thr^{202}/Tyr^{204}), GRP78/BiP, IRE-1α, H2B, insulin receptor β-subunit (IRβ) (Cell Signaling Technology Inc., Danvers, MA), IκBα, p65 (Santa Cruz) and actin (Sigma). Detection was achieved using the Western Lightning® Plus-ECL chemiluminescence kit (PerkinElmer, Waltham, MA, USA). The equal loading of proteins was assessed by Ponceau S staining. The size of proteins detected was estimated using protein molecular-mass standards (Bio-Rad).

Deoxy-D-glucose,2-[1,2-^{3}H(N)] uptake experiments Cells were starved for 24 h and washed twice with HEPES buffer (20 mmol/l HEPES [pH 7.4], 140 mmol/l NaCl, 2.5 mmol/l $MgSO_4$, 5 mmol/l KCl, 1 mM $CaCl_2$). Cells were preincubated with HEPES buffer for 1 h and incubated for 30 min in the presence or absence of 100 nmol/l insulin, followed by treatment with deoxy-D-glucose,2-[1,2-^{3}H(N)] (37,000 Bq/ml; Amersham Biosciences) for 20 min. The uptake was

stopped by adding 10 μmol/l cytochalasin B. After washing with ice-cold 0.9% NaCl three times, cells were lysed with 0.1 mol/l NaOH. Non-specific uptake was measured in the presence of 10μmol/l cytochalasin B and was subtracted from all the values.

High Performance Liquid Chromatography Measurement of AMP Adenine nucleotides were separated by high performance liquid chromatography using an X-Bridge column with a 3.5 μm outer diameter (100 x 4.6 cm). Elution was done with 0.1 mmol/l potassium dihydrogen phosphate, pH 6, containing 4 mmol/l tetrabutylammonium hydrogen sulphate and 15% (v/v) methanol. The conditions were as follows: 20 μl sample injection, column at room temperature, flow rate of 0.6 ml min^{-1} and UV monitoring at 260 nm.

1. Salvadó L, Coll T, Gómez-Foix AM, Salmerón E, Barroso E, Palomer X, Vázquez-Carrera M (2013) Oleate prevents saturated-fatty-acid-induced ER stress, inflammation and insulin resistance in skeletal muscle cells through an AMPK-dependent mechanism. Diabetologia 56: 1372-1382

Electronic supplementary material (ESM)-Table 1

Table 1. Primer sequences used for RT- PCR

Primers sequences used for real-time PCR		
Gene	**Primers**	
mAprt	for	5'-CAGCGGCAAGATCGACTACA-3'
	rev	5'-AGCTAGGGAAGGGCCAAACA-3'
hATF3	for	5`-AAGAACGAGAAGCAGCATTTGAT-3´
	rev	5`-TTCTGAGCCCGGACAATACAC-3´
mBip	for	5`-CAGATCTTCTCCACGGCTTC-3`
	rev	5`-GCAGGAGGAATTCCAGTCAG-3`
hCHOP	for	5`- GGAAATGAAGAGGAAGAATCAAAAAT-3`
	rev	5`-GTTCTGGCTCCTCCTCAGTCA-3`
mGrp94	for	5`-CATACCAGACGGGCAAGGA-3`
	rev	5`-TGATCAGTGGGTGTCTAGGATTGA-3`
mIl-6	for	5'-ACACATGTTCTCTGGGAAATCGT-3'
	rev	5'-AAGTGCATCATCGTTGTTCATACA-3'
hIL-6	for	5'-CCCCCAGGAGAAGATTCCAA-3'
	rev	5'-TCAATTCGTTCTGAAGAGGTGAGT-3'
mOrp150	for	5`-CACTGCACAGAACGTCATGTTCT-3`
	rev	5`-GGTGACGATGGTGCACACA-3`
mTnfα	for	5`-AGCCGATGGGTTGTACCTTGT-3`
	rev	5`-TGAGATAGCAAATCGGCTGAC-3`
h18S	for	5`-GCCGCTAGAGGTGAAATTCTTG-3`
	rev	5`-CATTCTTGGCAAATGCTTTCG-3`
Gene	**Primers**	
XBP1	for	5'-TGAGAACCAGGAGTTAAGAACACGC-3'
	rev	5'-TTCTGGGTAGACCTCTGGGAGTTCC-3'